



High stability in near-infrared spectroscopy: part 1, adapting clock techniques to optical feedback

Mathieu Casado, Tim Stoltmann, Amaelle Landais, Nicolas Jobert, Mathieu Daëron, Frederic Prié, Samir Kassi

► To cite this version:

Mathieu Casado, Tim Stoltmann, Amaelle Landais, Nicolas Jobert, Mathieu Daëron, et al.. High stability in near-infrared spectroscopy: part 1, adapting clock techniques to optical feedback. Applied Physics B - Laser and Optics, 2022, 128 (3), pp.54. 10.1007/s00340-022-07774-2 . hal-03598400

HAL Id: hal-03598400

<https://hal.science/hal-03598400>

Submitted on 31 Mar 2022

HAL is a multi-disciplinary open access archive for the deposit and dissemination of scientific research documents, whether they are published or not. The documents may come from teaching and research institutions in France or abroad, or from public or private research centers.

L'archive ouverte pluridisciplinaire **HAL**, est destinée au dépôt et à la diffusion de documents scientifiques de niveau recherche, publiés ou non, émanant des établissements d'enseignement et de recherche français ou étrangers, des laboratoires publics ou privés.

High stability in near-infrared spectroscopy: Part 1, adapting clock techniques to optical feedback

Mathieu Casado^{1,2,3}, Tim Stoltmann^{1,4}, Amaelle Landais², Nicolas Jobert⁵, Mathieu Daëron², Frederic Prié², Samir Kassi¹

¹ LiPHY, Laboratoire Interdisciplinaire de Physique, Université Grenoble Alpes / CNRS, Grenoble, France

² Laboratoire des Sciences du Climat et de l'Environnement, LSCE / IPSL, CEA-CNRS-UVSQ, Université Paris-Saclay

³ Now at: Alfred Wegener Institut Helmholtz Centre for Polar and Marine Research, Postdam, Germany

⁴ Now at: AP2E, Aix en Provence, France

⁵ ALMA Consulting, Arcueil, France

Received: date / Revised version: date

Abstract Optical feedback is an efficient way to narrow and stabilise semi-conductor lasers. As a step forward for ultra-stable, yet highly tunable sources, we developed a new prototype of a three-mirror V-shaped optical cavity (VCOF). It is made of a precisely machined Zerodur spacer, that holds 3 optical contacted mirrors forming a high finesse V-shaped cavity. This arrangement allows the resonant light to be sent back to the seeding laser, triggering a drastic narrowing of the emission linewidth well below the cavity mode width without the need for high-bandwidth active electronic lock of the laser on the cavity. Low expansion material and precise temperature control of the reference cavity leads to a source with Hz level frequency drift and 70 Hz-level

emission linewidth at 215 THz. We discuss the benefits of this new prototype compared to its predecessor for high-sensitivity cavity ring down spectroscopy (CRDS). To serve this purpose, the frequency stabilised laser was characterised on short, mid and long time scales, using a high finesse etalon, a self referenced optical frequency comb and a long term saturated CRDS absorption Lamb dip measurement on water.

1 Introduction

Laser absorption spectroscopy is a widely used method for fast and precise trace detection measurements in gas [1, 2]. Narrow and stable (in term of frequency deviation)

laser sources are crucial to reach the precision and accuracy requirements of high-precision spectroscopy, that have increased in the past years [3]. In particular, to achieve performances capable to distinguish different isotopes of the same molecule (such as water or carbon dioxide, relevant for environmental studies), extreme sensitivity levels are required [4–7]. The traditional continuous wave cavity ring down spectroscopy (cw-CRDS) [8, 9] relies on the coupling of a resonator with a monofrequency laser. **While for a single ring-down, the resonator maintains a fixed, high finesse frequency, the coupling of the resonator with the seeding light prevents an accurate determination of the frequency axis, and in turn, limit the precision of the spectroscopic measurement.** One way to stabilise a laser source is to remove the jitter of the laser with Pound-Drever-Hall (PDH) lock technique [10,11] that actively locks the laser frequency on a cavity, usually linear. It is common to use the CRDS cavity itself as a resonator to achieve efficient stabilisation of a **free-running** laser (FARS CRDS[12]). This locking scheme requires the laser source to have an already quite low frequency noise and is generally limited to expensive, and complex to drive tunable External Cavity Diode Laser [13] or poorly tunable pre-stabilised laser [14]. On the other hand, widely available distributed feedback laser diode (DFB) are rather broadly and easily tunable but suffer a high jitter noise, leading to MHz emission linewidth.

Optical feedback is an elegant method to improve the spectral properties of lasers such as distributed feedback diodes (DFB) [15]. The long term stability of an external reference cavity is transferred via direct optical feedback to the seeding laser, whose emission linewidth is narrowed well below the mode width of the seeded cavity. This well understood mechanism [16] has been exploited in Optical Feedback Cavity Enhanced Absorption Spectrometer (OFCEAS) setups [17], in fibre Bragg gratings [18] and V shaped Cavity Optical Feedback laser sources (VCOF) [15]. V-shaped cavities are classically used **to avoid unwanted feedback from** the reflection of the entry mirror, making it straightforward to obtain high level optical feedback from the cavity by only controlling the feedback phase with a slow PID servo loop (8 kHz bandwidth), acting on either a mirror actuated by piezoelectric or an electro-optic phase modulator (patented technology FR3056837B1). The linewidth and the stability of the laser are therefore linked to the thermo-mechanical properties of the cavity used for the optical feedback. In order to improve the thermal stability and the mechanical stiffness of the V-shaped cavity compared to previous models [15], and following classical designs of cavities made for atomic clocks [19,20], we used a monobloc Zerodur cavity on which the mirrors are optically contacted (see Fig. 1). As a result, the laser spectral purity and long term frequency stability were increased, even though without reaching atomic cavity stability level due to a sub-optimal, but very competitively priced, design.

2 Experimental setup

DFB laser

90% 10%

Isolator

EOM

Fibre coupling

Temperature stabilised vacuum chamber

photo diode

ν_n

servo loop

50% 50%

Optical frequency comb

$k f_{\text{rep}} + f_0$

Referenced to:

- GPS Absolute reference
- VCOF Previous setup
- OE wave Ultra narrow

Phase modulation

ν_n

$\nu_n + \nu_{\text{RF}}$

95% 5%

λ wavemeter

grating

photo diode

Fibre coupling

ν_n

$k f_{\text{rep}} - f_0$

50% 50%

High Finesse cavity

photo diode

Low Finesse cavity

photo diode

Frequency stabilisation

Optical feedback

Measurement techniques

- 1. Fizeau interferometry**
 $\nu_n \pm 20 \text{ MHz}$
- 2. Beatnote**
 $\nu_n - k f_{\text{rep}} - f_0$
 - 2.1 GPS**
 $\nu_n \pm 100 \text{ kHz}$
Virtually no drift
 - 2.2 VCOF**
 $\nu_n \pm 350 \text{ Hz}$
Drift: 9.3 Hz s^{-1}
 - 2.3 OE wave**
 $\nu_n \pm 100 \text{ Hz}$
Drift: 50 kHz s^{-1}
- 3. Saturated H_2O line**
 $\nu_n \pm 2 \text{ kHz}$
Physically based
- 4. FM to AM noise conversion**
 ΔA
 $\Delta \nu_n$
 $\nu_n \pm 1 \text{ Hz relative}$

cludes the first order dispersion due to the cavity mirrors [21]. With a flat linear fit residual (Fig. 2, upper pannel) over the 1 THz explored region, no sign of second order dispersion was evidenced.

The agility of the laser source is also demonstrated in a scan of the frequency of the DFB laser by changing its temperature (Fig. 2 bottom right panel): the

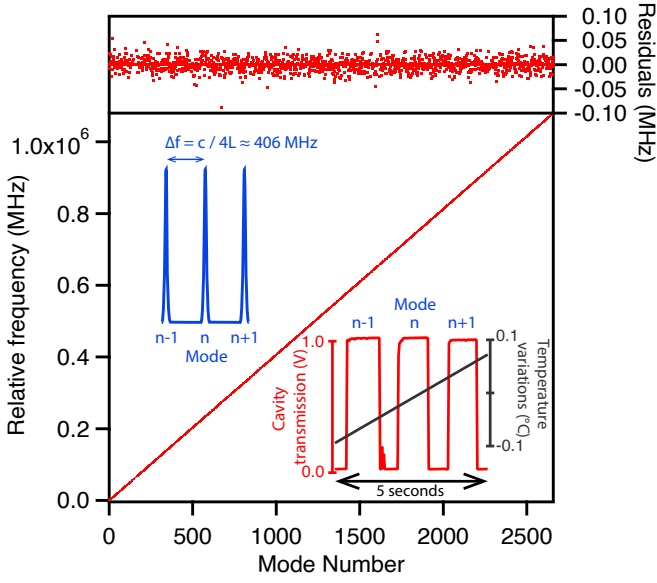


Fig. 2 Free spectral range estimated using the beatnote with the comb (method 2.1). The standard deviation of the measurement is roughly 10 kHz due to the wide linewidth of the comb teeth compared to the VCOF. Top left insert: illustration of the FSR of the cavity; bottom right insert: temporal zoom on the laser locking on successive mode while the temperature is scanned, the relock is instantaneous.

laser remains locked over a broad spectral region (locking range), until it delocks, being pushed too far from the resonant mode. In our experiment, we only scanned the temperature of the DFB, and as soon as the laser emission approaches the cavity modes, the automatic relock occurs, in the present setup, within a few hundreds of millisecond. The agility of the relock is not limited to slow scans, and similar performances can be achieved jumping a large number of modes (in this case, only limited by the response time of the DFB laser to temperature changes).

In order to limit thermal effects, the cavity is surrounded by a 5 mm thick copper shield damping the external temperature excursion. Moreover, the assembly is housed in a stainless steel vacuum enclosure pumped down to 10^{-8} mbar by a vibration-free ionic pumping system. Three wedged optical ports with anti-reflection coatings (two on the top and one on the bottom flange) allow the light to enter or exit the assembly. Note that a single window allows two beams to be extracted through the bottom flange, corresponding to the laser injection and feedback port.

As illustrated in Fig. 1, the V-shaped cavity is seeded using a modified fibred DFB laser Eblana EP1392. By using polarisation maintaining fibres, optical feedback is achieved as straightforwardly as with a free space diode. This technique, already used in fibre gratings [18], was never successful for external cavities and relies on the combined used of polarisation maintaining fibres, the absence of optical isolator in front of the laser, and active phase correction. The laser-cavity distance is controlled using a fibred Electro-Optic Modulator (EOM) taking into account slow phase drifts of the feedback path length. Practically, we apply a weak 50kHz modulation to the EOM to determine with the help of a lockin amplifier the relative phase between the laser and the cavity [15]). We have evaluated the performance of this new optical feedback laser source by combining several optical setups to evaluate the spectral properties over time scales from the ms to several days. The most

straightforward approach to evaluate the performances of the system would be to do a beatnote with two replicates laser sources which could not be achieved. Instead, we use several approaches allow for precise frequency measurement at both short and long time scales. Commercial wavemeters are limited to an accuracy of a few MHz over a limited period (hours), which makes them too inaccurate for an extensive characterization, but permits to unambiguously identify which V cavity mode is acting. Nevertheless, in combination with the beatnote obtained by mixing the laser with a GPS-referenced optical frequency comb (MENLO FC1500), determination of the absolute frequency can be refined down to a few Hz (measurement technique 2.1. in Fig 1) [22]. In Fig. 3 the frequency deviation of the DFB laser stabilised against the optically contacted cavity (red curve) is presented in comparison with a range of commercial tunable lasers (the grey area encompasses the temperature stabilised DFB diode, top edge, and the free-running ECDL, bottom edge). Without optical feedback, DFB laser sources are typically MHz broad and start drifting within 100 ms. For a room temperature and free-running ECDL (among the narrow widely tunable laser sources), we can see that the Allan variance decreases down to 20 kHz after 0.1 s before thermomechanical drifts take over (bottom grey curve in Fig. 3). For the DFB laser locked on the VCOF, we observe that the Allan variance decreases following a $N^{-1/2}$ ergodic law. A minimum deviation of 341 Hz is reached after 110 s. The rising

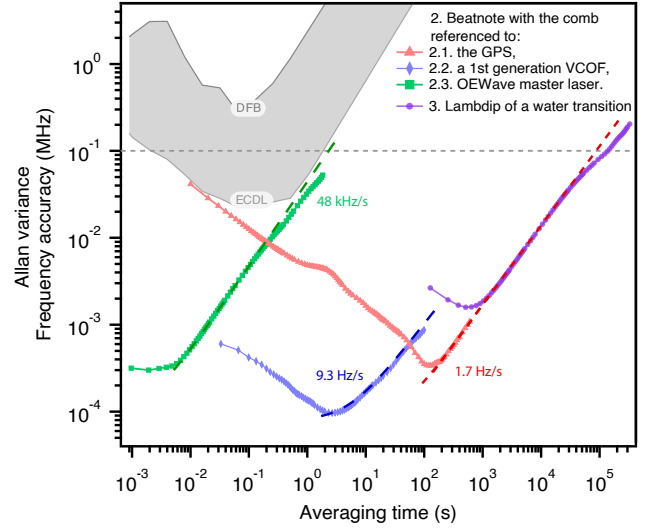


Fig. 3 Comparison of the Allan variance of the frequency of a DFB locked on the VCOF measured by the beatnote with a tooth of the comb locked on 2.1 a GPS (red triangles), 2.2 a first generation VCOF (blue diamonds), 2.3 an OEWave laser (green squares) or by using the center of a Lamb dip of a saturated absorption (method 3, purple). The grey area illustrates the range of stability for common tunable laser sources (top, DFB laser, bottom, ECDL).

slope of $1.7 \text{ Hz} \cdot \text{s}^{-1}$ observed after 110 s gives an estimate of the long term drift of the cavity. It is about 10 times more stable than the previous generation of VCOF [15].

3 Frequency deviation

One of the measurement limits here is that the linewidth of each tooth of the GPS disciplined optical frequency comb (OFC) is intrinsically much larger than the VCOF emission linewidth, leading to an apparent noise excess of 100 kHz. To overcome this limitation, we have repeated the measurement with the OFC being optically locked

to a VCOF of a previous generation (measurement technique 2.2. in Fig 1), similar to the one in the study of [15]. We obtained an increased combined drift (9.3 Hz s^{-1}), but a much lower short-time combined noise (600 Hz) and a lower variance minimum (96 Hz), confirming the ability of VCOF cavities to be used for determining frequencies with a precision better than 100 Hz within one second (blue curve 2.2 in Fig. 3). Due to its composite mechanical structure, the old VCOF setup was prone to frequency noise, which was stated to be on the order of 600 Hz [15]. We thus estimate that the short-time combined noise is dominated by the old VCOF setup short term noise.

In order to confirm this hypothesis, the OFC was locked to a narrow linewidth commercial laser OEwave (measurement technique 2.3. in Fig 1). We obtained a short term combined noise of 317 Hz but a fast 48 kHz s^{-1} drift of the Allan variance curve (green trace in Fig 3). The flat Allan variance during the first 10 ms indicates that noise from one of the lasers is dominating. Considering that the blue trace goes below 100 Hz , one concludes that the OEwave is responsible for the drift. Since in experiment 2.2, the OFC was locked at 1550 nm while the VCOF emission is at 1400 nm , part of the short term noise may be due to incomplete coherence transfer from tooth to tooth [23]. One may conclude that the short term noise excess of the old VCOF version is between 300 and 600 Hz (blue curve), and that the one of the new VCOF is below 300 Hz . For the drifts, we put forward

that the EOWave, Old VCOF and new VCOF drift by about 50 kHz s^{-1} (green curve), 10 Hz s^{-1} (blue curve) and 2 Hz s^{-1} (red curve), respectively.

To confirm the results, another method was used to independently assess these performances: we carried out an Allan Variance study of the VCOF drift monitoring a molecular absorption line. We recorded a Lamb dip feature of a strong water line over several days [22]. The Lamb dip [24, 22] is a narrow peak that shows up at the center of the Doppler limited absorption (measurement technique 3. in Fig 1). It has a sufficiently narrow signature to allow for a centre determination with 2 kHz frequency accuracy. This is presented in purple in Fig. 3. Lamb dip measurements provide an independent measurement of the long term behaviour of the cavity and confirm drift level below 2 Hz.s^{-1} . Note that the drift of the cavity length (and in turn of the frequency) is not monotonous over a timescale on the order of a day, but oscillates around an equilibrium position. Thus, over several days, the frequency deviations are limited to 100 kHz , leading to a drift below 0.3 Hz.s^{-1} for time scales longer than 10^5 s . This was confirmed by a two-year regular monitoring of the Lamb dip feature indicated that the aging of the assembly was $0.73 \pm 0.09 \text{ Hz.s}^{-1}$, typical for Zerodur assemblies [25].

As a final attempt to evaluate the intrinsic noise of the cavity, we injected the laser in a relatively low finesse cavity (approximately 13500), used as a frequency etalon (measurement technique 4. in Fig 1). Indeed, at

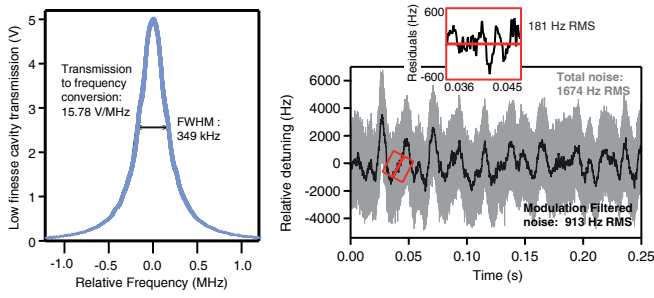


Fig. 4 Evaluation of the linewidth of the VCOF with a low finesse etalon: left, scan of the etalon transmitted power over 2.4 MHz, right, relative detuning of the VCOF obtained by converting the power fluctuation into frequency fluctuation with a slope of 15.78 V MHz^{-1} (raw conversion, grey curve), filtering the high-frequency modulation used to lock the cavity (low-pass filtered, black curve), and zooming on the substructure associated solely with the VCOF frequency variation (red inset).

the half-maximum of the transmission peak of the low finesse cavity, the variation of the transmission with the laser optical frequency is locally linear ($r^2 = 0.98$). As a result, the frequency noise of the injected light is converted in transmitted power variations (see Fig. 4). Obviously, this method is limited by the thermomechanical fluctuations of the etalon cavity length that shifts its resonant frequency and the 10 m long unstabilised fibre link from the VCOF to the cell [26,27]. A typical transmitted power trace is given in Fig. 4. The raw data (grey curve, right panel) includes the high-frequency modulation applied to maintain the laser light locked to the VCOF (see Section 2). This high-frequency modulation (50 kHz) can be filtered out to obtain the actual intrinsic noise of the light produced by the V-shaped cavity.

We observe that the standard deviation of the frequency excursion is 913 Hz, once the modulation implemented to lock the laser source in the low finesse etalon has been filtered. This value is larger than expected considering the finesse of the cavity, as previously mentioned. Additionally, there seems to be a narrower structure inside the relatively slow oscillations observed in the time series. Assuming the large excursions are due to the etalon and the fibre link, which is justified according to the upper linewidth set by the green curve in Fig. 3, only a 181 Hz RMS excursion would be associated with the VCOF, as shown in the zoom part (red inset).

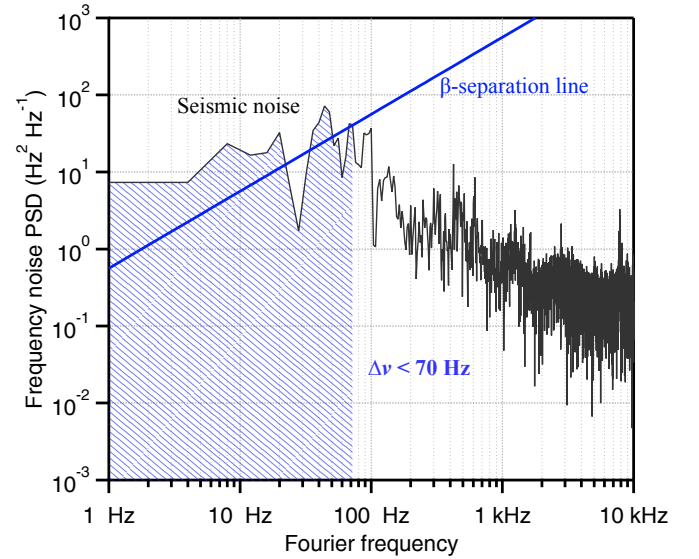


Fig. 5 Frequency noise PSD of the VCOF with a frequency etalon. The shaded area A corresponds to a laser linewidth $\Delta\nu = \sqrt{8 \ln 2 A}$ [28, 15].

Using the beta-separation line technique [28], we estimate which part of the noise is linked to the intrinsic noise of the VCOF (below 70 Hz, blue area in Fig. 5)

and contributes to the laser linewidth, and which part of the noise does not contribute to the linewidth (more than 100 Hz). As for [15], the laser frequency noise is most likely to be lower than what we obtain here as we combine the noise of both the etalon and the VCOF. These results suggest that the laser full width at half-maximum (FWHM) is below 70 Hz , almost one order of magnitude narrower than the previous VCOF [15], narrowing by more than four orders of magnitude the DFB laser used as a source. While this figure is much larger than what is presently achieved by atomic clocks or some commercial lasers such as the EOwave, combined with a very low drift and a tunability across several THz, this source reaches unique performances that, for instance, enable to study hyperfine structures within molecular transition [22], and thus provide a referenced laser source that can be used for optical spectroscopy out of a laboratory.

Overall, the vibrational study [29] predicts that at this time scale, the frequency excursions of the VCOF should be within 10 to 100 Hz , which concurs with our experimental results. On the other hand, the drift predicted by the mechanical study carried out for this setup, mainly aging and temperature fluctuations, are expected to be smaller than observed. To evaluate the temperature sensitivity of the cavity, we proceeded to an abrupt temperature step of 0.96 K of the regulation box set-point (normally temperature controlled within 10mK). Figure 6 indicates that the frequency response of the

cavity (around 11 MHz) is much larger than expected from the Zerodur thermal expansion coefficient (around 2 MHz). This can be partly explained by thermally-induced stress deforming the mirror curvature, and subsequently affecting the resonance frequencies of the cavity modes [29]. Note that the introduction of a massive copper shield introduced a much longer response time (almost 36 hours) of the system to external temperature fluctuations than for the previous system. Coupled with the higher performances of the cavity (11 MHz/K against more than 100 MHz/K for previous generations [15]), this leads to low level of drift, and thus this system does not require routine frequency referencing. In particular, combined with active temperature stabilisation of the vacuum enclosure (within 10mK), the frequency drift of the cavity remains below 2 Hz.s^{-1} even if the temperature stabilisation of the environment exceed 1 K , with maximum daily excursion around 50 kHz . As such, it is therefore a big step towards field-deployable very narrow, yet broadly tunable, laser sources, that should fulfil requirements for most field spectroscopy campaign purposes.

4 Conclusion

To sum up, we have characterised a new iteration of a V-shaped Cavity stabilising a laser by Optical Feedback, with very stable frequency stability (below 2 Hz.s^{-1}), a very narrow linewidth (below 100 Hz), and high power efficiency (more than 80% of the light being available

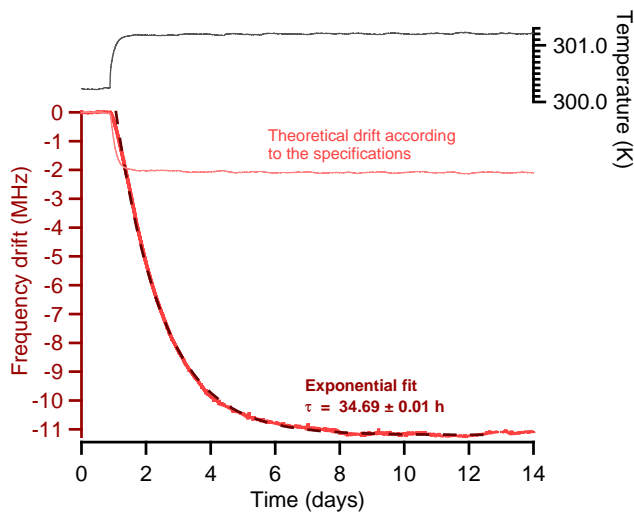


Fig. 6 Evaluation of the drift of the cavity for a temperature shift of 1 K: time series of the temperature on the external flange (black line), frequency drift measured by beatnote with the OFC (red thick line), exponential fit of the variations (dark red dashed line), and expected drift according to the specifications of the Zerodur spacer (light red line).

for applications). The Optical Feedback was achieved through fibre coupling. The laser-cavity optical distance was controlled with a fibred electro-optic phase modulator (EOM) acting as an optical distance modulator. In addition to the DC correction signal, a low-exursion 50 kHz modulation was applied to the EOM. This induced a modulated transmission signal that was used to infer the DC correction to be applied by the servo loop in order to keep the laser and the cavity at the ideal optical cavity, modulo 2π . Finally, this enables to obtain rapid (less than 100 ms to lock) and stable through time (the laser can remain locked without adjustments) optical feedback on the DFB diode.

This new laser source is intended to be used for high precision spectroscopy (for example to be injected into a CRDS cavity [30,6]), or even in laboratories not equipped with a comb to measure absolute frequency. In the field, making use of the low drift value, and measuring the Lamb dip of a known transition, this temperature stabilised laser source can be used as a frequency reference. Alternatively, coupled to an optical frequency source, it can be used to retrieve accurate optical frequencies or improve the comb linewidth to transfer its high coherency to sources over a large range of wavelengths [23].

References

1. P. Werle, *Spectrochimica Acta Part A: Molecular and Biomolecular Spectroscopy* **54**(2), 197 (1998)
2. E. Kerstel, L. Gianfrani, *Applied Physics B* **92**(3), 439 (2008)
3. J.M. Hartmann, H. Tran, R. Armante, C. Boulet, A. Campargue, F. Forget, L. Gianfrani, I. Gordon, S. Guerlet, M. Gustafsson, J.T. Hodges, S. Kass, D. Lisak, F. Thibault, G.C. Toon, *Journal of Quantitative Spectroscopy and Radiative Transfer* (2018)
4. J. Landsberg, D. Romanini, E. Kerstel, *Optics Letters* **39**(7), 1795 (2014). DOI 10.1364/OL.39.001795. URL <http://ol.osa.org/abstract.cfm?URI=ol-39-7-1795>
5. E.J. Steig, V. Gkinis, A.J. Schauer, S.W. Schoenemann, K. Samek, J. Hoffnagle, K.J. Dennis, S.M. Tan, *Atmos. Meas. Tech.* **7**(8), 2421 (2014). DOI 10.5194/amt-7-2421-2014. URL <http://www.atmos->

- 10 Mathieu Casado, Tim Stoltmann, Amaelle Landais, Nicolas Jobert, Mathieu Daëron, Frederic Prié, Samir Kassi
meas-tech.net/7/2421/2014/ <http://www.atmos-meas-tech.net/7/2421/2014/amt-7-2421-2014.pdf>
6. T. Stoltmann, M. Casado, M. Daëron, A. Landais, S. Kassi, *Analytical chemistry* **89**(19), 10129 (2017)
 7. M. Casado, Water stable isotopic composition on the East Antarctic Plateau: measurements at low temperature of the vapour composition, utilisation as an atmospheric tracer and implication for paleoclimate studies. Ph.D. thesis, Paris Saclay (2016)
 8. D. Romanini, P. Dupre, R. Jost, *Vibrational spectroscopy* **19**(1), 93 (1999)
 9. P. Macko, R. Plašil, P. Kudrna, P. Hlavenka, V. Poterya, A. Pysanenko, G. Bánó, J. Glosik, *Czechoslovak Journal of Physics* **52**(2002 Suppl D), D695 (2002)
 10. R.V. Pound, *Review of Scientific Instruments* **17**(11), 490 (1946)
 11. R.W.P. Drever, J.L. Hall, F.V. Kowalski, J. Hough, G.M. Ford, A.J. Munley, H. Ward, *Applied Physics B* **31**(2), 97 (1983)
 12. G.W. Truong, K.O. Douglass, S.E. Maxwell, R.D. van Zee, D.F. Plusquellic, J.T. Hodges, D.A. Long, *Nature Photonics* **7**, 532 (2013). URL <https://doi.org/10.1038/nphoton.2013.98> 10.1038/nphoton.2013.98
 13. J.T. Hodges, R. Ciuryło, *Review of scientific instruments* **76**(2), 23112 (2005)
 14. V. Crozatier, F. De Seze, L. Haals, F. Bretenaker, I. Lorgère, J.L. Le Gouët, *Optics communications* **241**(1-3), 203 (2004)
 15. J. Burkart, D. Romanini, S. Kassi, *Optics letters* **38**(12), 2062 (2013)
 16. P. Laurent, A. Clairon, C. Breant, *Quantum Electronics, IEEE Journal of* **25**(6), 1131 (1989)
 17. J. Morville, S. Kassi, M. Chenevier, D. Romanini, *Applied Physics B* **80**(8), 1027 (2005). DOI 10.1007/s00340-005-1828-z. URL <http://dx.doi.org/10.1007/s00340-005-1828-z>
 18. F. Wei, F. Yang, X. Zhang, D. Xu, M. Ding, L. Zhang, D. Chen, H. Cai, Z. Fang, G. Xijia, *Optics express* **24**(15), 17406 (2016)
 19. A.D. Ludlow, X. Huang, M. Notcutt, T. Zanon-Willette, S.M. Foreman, M.M. Boyd, S. Blatt, J. Ye, *Optics Letters* **32**(6), 641 (2007). DOI 10.1364/OL.32.000641. URL <http://ol.osa.org/abstract.cfm?URI=ol-32-6-641>
 20. J. Millo, D.V. Magalhaes, C. Mandache, Y. Le Coq, E.M.L. English, P.G. Westergaard, J. Lodewyck, S. Bize, P. Lemonde, G. Santarelli, *Physical Review A* **79**(5), 53829 (2009)
 21. L. Rutkowski, A.C. Johansson, G. Zhao, T. Hausmaninger, A. Khodabakhsh, O. Axner, A. Foltynowicz, *Optics express* **25**(18), 21711 (2017)
 22. S. Kassi, T. Stoltmann, M. Casado, M. Daëron, A. Campargue, *The Journal of Chemical Physics* **148**(5), 54201 (2018). DOI 10.1063/1.5010957. URL <https://doi.org/10.1063/1.5010957>
 23. R. Gotti, T. Sala, M. Prevedelli, S. Kassi, M. Marangoni, D. Romanini, *The Journal of Chemical Physics* **149**(15), 154201 (2018). DOI 10.1063/1.5046387. URL <https://doi.org/10.1063/1.5046387>
 24. J. Burkart, T. Sala, D. Romanini, M. Marangoni, A. Campargue, S. Kassi, *The Journal of chemical physics* **142**(19), 191103 (2015)

25. R.W. Fox, B.R. Washburn, N.R. Newbury, L. Hollberg,
Applied optics **44**(36), 7793 (2005)
26. J. Ye, Q. Li, S.Q. Peng, Y.L. Chen, Applied optics
29(12), 1724 (1990)
27. L.S. Ma, P. Jungner, J. Ye, J.L. Hall, Optics letters
19(21), 1777 (1994)
28. G. Di Domenico, S. Schilt, P. Thomann, Applied Optics
49(25), 4801 (2010). DOI 10.1364/AO.49.004801. URL
<http://ao.osa.org/abstract.cfm?URI=ao-49-25-4801>
29. N. Jobert, M. Casado, S. Kass, Applied Physics B **Un-
der revi**
30. J. Burkart, S. Kass, Applied Physics B **119**(1),
97 (2015). DOI 10.1007/s00340-014-5999-3. URL
<http://dx.doi.org/10.1007/s00340-014-5999-3>